Pergamon

Solid-State Electronics Vol. 42, No. 9, pp. 1761–1763, 1998

0038-1101/98/$ - see front matter

PII: S0038-1101(97)00280-3

LETTER

THE TUNNEL DIODE AS A THYRISTOR EMITTER

Z.S. GRIBNIKOV*, V.A. KOROBOV and V.V. MITIN

Department of Electrical and Computer Engineering, Wayne State University, Detroit, MI 48202, U.S.A.

(Received 19 July 1997; accepted 17 September 1997)

Abstract—We propose a tunnel switching mechanism for a thyristor. This mechanism can be realized if a tunnel pn-junction is used as the thyristor emitter. The switching current is fully determined by a junction peak tunnel current and weakly depends on temperature. Thus stabilization of the thyristor's switching and holding currents can be accomplished in a new way. The device voltage exhibits discontinuities as the device turns on. Results of numerical simulation of the tunnel emitter's effects on the thyristor's I–V characteristics are presented. © 1998 Elsevier Science Ltd. All rights reserved

Key words—Thyristor, Tunnel diode, Semiconductor device simulation

Tunnel diodes are semiconductor devices, well known as negative resistance circuit elements with N-type current–voltage characteristics in the forward direction. They also serve as suitable connection elements in multijunction semiconductor device structures (for example, in solar cells[1]). We propose a novel application of the tunnel p^+n^--junction for a thyristor design. In this application the tunnel junction with an N-like forward I–V characteristic is used as one of the thyristor emitters (i.e. as one of the outer thyristor junctions).

It is known[2] that the thyristor S-type I–V characteristic is the result of a combination of two different factors. First, a mechanism which provides a current growth at some critical breakover voltage V_b must be available; current usually increases due to avalanche multiplication in the middle (collector) junction of the device and/or punch-through of the lightly doped thyristor base. Second, an increase of injection efficiency of thyristor emitters from almost zero values to values close to unity, is another necessary condition for thyristor switching. Currently there are two known mechanisms by which the efficiency increases with injection: (1) Sah–Noyce–Shockley (SNS) recombination[3] through deep centers in the transition region of the emitter junction and (2) emitter shorts[2], which serve as shunts of the emitter junctions at small biases.

In this paper we consider a third mechanism of injection efficiency increase with the device current. This mechanism takes place if a heavily doped p^+n^+-junction with a tunneling N-type current voltage characteristic is built up at the transition region between the outer region of the device and one of the thyristor bases (that means that instead of a traditional p^+npn^+ device we consider a $(p^+n^+)npn^+$ or $p^+np(p^-n^+)$ structure). The latter multilayer structure can be obtained by utilizing fine growth techniques such as molecular beam epitaxy, metalorganic chemical vapor deposition, or other "layer by layer" methods of crystal growth.

A typical current–voltage characteristic of the tunnel diode emitter is shown in the insert in Fig. 1. The peak and valley currents J_p, J_v and the valley voltage V_v depend on doping concentrations of the p^+n^+ tunnel junction, the type of material the junction is made of, and the magnitude of excess currents[4]. For brevity we will refer to current densities J, J_p, J_c, and J_v as currents. In the one-dimensional problem we are dealing with, this fact should not cause confusion. The current in region 1 of the tunnel diode characteristic flows solely due to Zener's band-to-band tunneling. At the same time the thyristor action requires the injection of minority carriers into the bases. Obviously, the needed injection is negligible in portion 1 of the curve because the tunneling current is much larger than the diode injection current. This means that the injection efficiency γ_1 of such an emitter is close to zero at small forward biases. An increase in current J due to avalanche or punch-through of the second base (not adjacent to the tunnel emitter) does not change γ_1 and in the whole range $0 < J < J_p$ the tunneling current still dominates over the recombination and injection components of the total junction current. When the current achieves the peak value J_p, a transition a–b occurs and the voltage V across the junction suddenly increases to $V_0 = V(J_p)$. We will distinguish two situations. First, at the point where $J = J_p$ and $V = V_0$, the efficiency γ_1 is controlled by the SNS recombination. This means that the current J_p is less than J_c — the critical current at which injection starts to dominate over recombination within the emitter transition region. That happens at such voltages V_1 across the junction when the injection component $J_{in}^{I} \sim \exp(V_1/kT)$ of the diode current becomes greater than recombination component $J_r \sim \exp(V_1/2kT)$. In the case $J_p < J_c$ the specific features of the N-type junction I–V characteristic are not important. We are mostly interested in the other situation, when at the point $J = J_p$ and $V = V_0$ the injection component of the current exceeds the recombination current (i.e. $J_p > J_c$). In this case the result of the transition a–b is an instant increase of the emitter efficiency from 0 to almost 1. If at this point efficiencies γ_1 and γ_2 of the two outer junctions and emitter-to-collector current transfer ratios α_1 and α_2 satisfy the condition $\gamma_1\alpha_1 + \gamma_2\alpha_2 > 1$ the thyristor turns on at $J = J_p$ and the voltage across the

*Corresponding author.

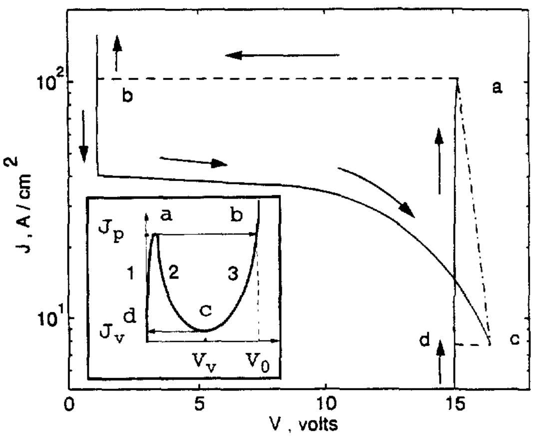

Fig. 1. Current–voltage characteristic of a symmetric thyristor with two tunnel junctions. At $J = J_p = 100$ A/cm^2 the emitter efficiency jumps from 0 to 1 as a result of transition a–b. At $J = J_v = 7.5$ A/cm^2 the device voltage suddenly decreases. A schematic view of the tunnel diode I–V characteristic is shown in the insert

device suddenly drops down. Further increase in current will cause the voltage across the junction to grow according to branch 3 of the I–V curve. It is interesting to note that if the current decreases below J_p due to the external circuit, the voltage does not exhibit any discontinuities at $J = J_p$ and at some holding current the device turns off according to the usual switching mechanism. Only at $J = J_v$ the voltage across the junction exhibits a discontinuity c–d. The less the difference between J_c and J_v the more abrupt is the device turnoff.

To illustrate the effect of the tunnel emitter on thyristor behavior we performed a numerical simulation of the device's static I–V characteristics. Assuming low injection levels in both bases, the solution of the continuity equation for concentrations of excess minority carriers (for example for a concentration of excess holes $p(x)$ in the n-base) may be written as

$$p(x) = p_0 \cdot [ch(\lambda_p x) - cth(\lambda_p W_n) sh(\lambda_p x)] + p_{W_n} \cdot \frac{sh(\lambda_p x)}{sh(\lambda_p W_n)} \quad (1)$$

Here λ_p is the inverse recombination length of holes, W_n is the n-base width. p_0 and p_{W_n} are the boundary hole concentrations, which can be written in terms of the junction voltages V_1 of the emitter 1 and V_c of the collector junction: $p_0 = p_{eq}(\exp(V_1/kT) - 1)$, $p_{W_n} = p_{eq}(\exp(-V_c/kT) - 1)$. p_{eq} is the equilibrium hole concentration in the n-base. Material parameters correspond to GaAs. Similar expressions hold for excess electron concentration $n(x)$ in the p-base, which has a width W_p. Emitter-to-collector current transfer ratios are $\alpha_1 = 1/ch(W_n \lambda_p)$ and $\alpha_2 = 1/ch(W_p \lambda_n)$.

The boundary conditions for the continuity equations are given by:

$$J = -qD_p \frac{dp}{dx} + J_{r1}(V_1) + J_{tun(1)}(V_1) \quad (2)$$

at the emitter junction 1 ($x = 0$):

$$J = M(V_c) \cdot \left[qD_n \frac{dn}{dx} - qD_p \frac{dp}{dx} + J_{gen}(V_c)\right] \quad (3)$$

at the collector junction (at $x = W_n$) and

$$J = qD_n \frac{dn}{dx} + J_{r2}(V_2) + J_{tun(2)}(V_2) \quad (4)$$

at the emitter junction 2 ($x = W_n + W_p$).

In Equations (2)–(4) q is the electron charge, D_n and D_p are electron and hole diffusion coefficients. The currents J_{r1} and J_{r2} due to recombination in emitters 1 and 2 and the current J_{gen} due to generation in the collector junction, were calculated using SNS model[3,4]. The carrier multiplication factor $M(V_c)$ of the middle junction and the emitter's tunnel currents were taken in the following empirical forms[2,4]:

$$M(V_c) = \frac{1}{1 - (V_c/V_b)^n} \quad (5)$$

$$J_{tun(1),(2)}(V_{1,2}) = J_p \cdot (V_{1,2}/V_p) \cdot \exp(1 - V_{1,2}/V_p), \quad (6)$$

where V_b is a breakover voltage of the collector junction, n is a factor equal to 5 in the simulation. Taking into account Equation (1), the system of Equations (2)–(4) was solved numerically to determine V_1, V_2, V_c as well as the device voltage drop $V = V_1 - V_c + V_3$ for a given value of the total current density J. Current voltage characteristics, shown in Figs 2–3 are obtained as a result of direct numerical solution of Equations (2)–(4). We use injection efficiencies γ_1 and γ_2 as well as transfer ratios α_1 and α_2 only for a qualitative description of the results in the discussion below.

Figure 1 demonstrates the results of numerical simulation for a symmetrical thyristor with $\alpha_1 = \alpha_2 = 0.93$. Currents J_p, J_v and J_c are 100 A/cm^2, 7.5 A/cm^2 and 38 A/cm^2. It is seen from Fig. 1 that there are two abrupt changes of the device voltage at $J = J_p$ and $J = J_v$. There is also branch c–a of the current–voltage dependence which corresponds to the region 2 in the insert in Fig. 1. The question about realization and stability of this branch needs further investigation. Branch a–c does not occur under the condition of slow (adiabatic) increase or decrease in current J. The transition into this branch could happen as a result of current fluctuations or under the influence of a pulsed current signal. The stability of the c–a portion of the I–V curve depends on the relationship between the negative differential conductivity of the tunnel p^+n^+-junction in region 2 (insert in Fig. 1) and the positive resistances of other thyristor's elements, and the external circuit. If the positive resistances are high enough branch c–a is unstable.

If a thyristor has only one tunnel junction, adjacent to the base 1, then device behavior may be substantially different, because the device I–V curve depends mostly on parameters α_2 and γ_2 of the second base when the junction

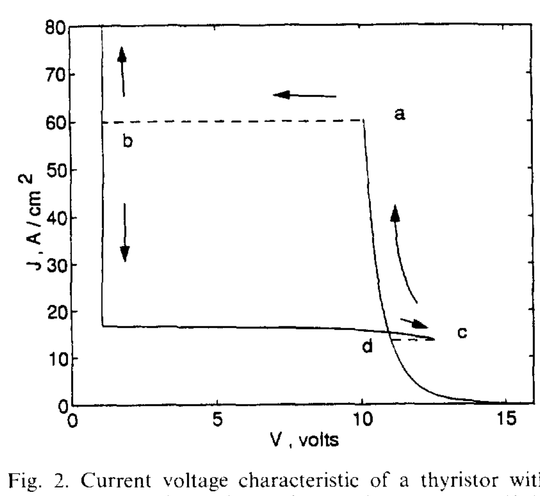

Fig. 2. Current voltage characteristic of a thyristor with one tunnel junction. The peak tunnel current $J_p = 60$ A/cm^2 is greater than $J_{c(1)} = 16$ A/cm^2 and $J_{c(2)} = 0.05$ A/cm^2. The second breakover voltage is $V \approx 12$ V

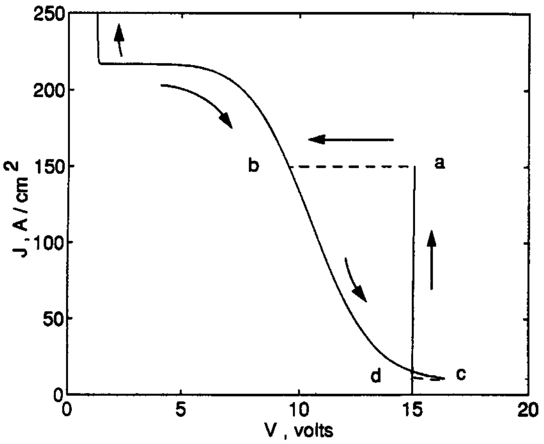

Fig. 3. I–V characteristic of an asymmetric thyristor with one tunnel junction. Transistor gains are $\alpha_1 = 0.13$, $\alpha_2 = 0.98$. At $J = J_p = 150$ A/cm^2 there is a transition a–b to the second branch of the I–V curve. Minimal current on the second branch is equal to $J_v \approx 10$ A/cm^2. At 8 V < V < 12 V there is a region of large negative differential conductivity. At V < 1.2 V the device is in the ON state

1 is in the tunneling regime. The second device breakover may take place in this case. Figure 2 shows simulated results for an asymmetric p^+npn^+ structure where only the left junction is tunneling (i.e. $J_{tun2} = 0$ in Equation (4)). Parameters J_p and J_v are 60 A/cm^2 and 13 A/cm^2. Currents $J_{c(1)}$ and $J_{c(2)}$ for the left and right junctions are $J_{c(1)} \approx 16$ A/cm^2 and $J_{c(2)} \approx 0.05$ A/cm^2, i.e. current J_p exceeds both $J_{c(1)}$ and $J_{c(2)}$. Transistor gains are $\alpha_1 = 0.95$ and $\alpha_2 = 0.98$. The first increase in the device current (not seen in Fig. 2) takes place at $V = V_b \sim 15$ V due to avalanche multiplication in the collector junction. At $J_{c(2)} < J < J_p$ the behavior of the I–V curve is determined by the approximate relationship $\gamma_2\alpha_2M_2 \approx 1$, where M_2 is a multiplication factor for carriers, injected by the second emitter. At $\gamma_2 = 1$ (this corresponds to the voltage $V \approx 12$ V in Fig. 2) the second breakover takes place where multiplication is still in effect and $M_2 = 1/\alpha_2$. Using Equation (5) the voltage V_{b2} across the middle junction at the beginning of the second breakover can be found as $V_{b2} = V_b(1-\alpha_2)^{1/n}$. The effect of the second breakover is well pronounced when the peak current J_p far exceeds $J_{c(2)}$ (this is the reason why $J_{c(2)}$ was chosen so low to obtain the results shown in Fig. 2). Note that this effect takes place if α_2 is close to unity, because the smaller α_2, the closer the second breakover voltage is to $V_b = 15$ V. The current–voltage characteristic, shown in Fig. 2 becomes similar to the curve shown in Fig. 1 at small enough α_2 ($\alpha_2 \approx 0.6$–0.7). We can say that α_2 controls the shape of the I–V characteristic in the considered situation.

If the current J_c for the junction 2 is greater than J_p we obtain a current–voltage characteristic, shown in Fig. 3. The simulation was performed for $\alpha_1 = 0.13$, $\alpha_2 = 0.98$, $J_p = 150$ A/cm^2, $J_v = 10$ A/cm^2, $J_{c(1)} = 15$ A/cm^2, $J_{c(2)} = 215$ A/cm^2. It is seen that besides the first breakover due to avalanche at $V = 15$ V there is a region at 8 $V < V <$ 12 V where current J noticeably increases with the decrease in V. At $J > J_p$ we have $\gamma_1 = 1$ and $\gamma_2\alpha_2M_2 + \alpha_1M_1 \approx 1$. It can be easily shown that second breakover voltage decreases as α_1 approaches 1. The type of the I–V curve shown in Fig. 3 is obviously not desirable for switching purposes and the optimal relationship is $J_p > J_{c(1)}$, $J_{c(2)}$. Regions similar to c–a in Fig. 1, can be plotted also in Figs 2 and 3. However, we did not simulate these regions, because some work needs to be done to answer a question about their practical realization.

In conclusion, we would like to note that the use of tunnel diodes as thyristor emitters may give some advantages over the traditional thyristor design. This is the case, for instance, when the SNS mechanism is not effective because of difficulties in controlling the concentration of deep recombination centers during the growth of the thyristor's pn junctions. A similar situation may occur at high temperatures, especially when thyristor bases are made from narrow band gap materials. Tunnel emitters may also be used when the technique of emitter shorts is not applicable, e.g. in thyristors with small junction cross areas (for example, light-emitting thyristors for smart pixels[5,6]). Being added to a thyristor structure, the role of the heavily doped p^+n^+ junction may be twofold. First, they will control the junction behavior at small currents as was described above. Second, their function will be to prevent the thyristor n^+n-base punch-through in the OFF state at such voltages, when the collector depletion region almost reaches the emitter junction. Thus, use of the tunnel junctions can also help in the optimization of trade-off between the device high blocking capabilities in the OFF state and low voltage drop in the ON state. Another useful feature of the tunnel emitters, important for thyristor realizations, is related to a weak dependence of the peak tunnel current J_p on temperature. That specific feature of the tunnel I–V characteristics (in conjunction with potentially high values of J_p up to 1000 A/cm^2[4]) may essentially expand the range of thyristor operating temperatures.

Acknowledgements—The authors wish to thank J. Petersen for reading of this manuscript. This work was supported by the NSF.

REFERENCES

1. T. Takamoto, E. Ikeda and H. Kurita, *Appl. Phys. Lett.* **70,** 381 (1997).
2. P. D. Taylor, *Thyristor Design and Realization*, J. Wiley, New York, 1987.
3. C. T. Sah, R. N. Noyce and W. Shockley, *Proc. IRE* **45,** 1228 (1957).
4. S. M. Sze, *Physics of Semiconductor Devices*, 2nd edn, J. Wiley, New York, 1981.
5. G. W. Taylor, P. A. Evaldsson, P. A. Kiely, T. Wang, P. R. Claisee, S. L. Daryanani, D. P. Docter, S. K. Sargood and P. W. Cooke, *IEEE J. Quantum Electron.* **29,** 785 (1993).
6. K. Kasahara, *IEEE J. Quantum Electron.* **29,** 757 (1993).